

The LiF used for the targets was (C.P.) Baker's analyzed. The known impurities are either incapable of producing neutrons in the energy range considered, or produce them in quantities insufficient to account for the observed peaks.

We may summarize by saying that in the neutron spectra obtained from the reaction $\text{Li}^7(p,n)\text{Be}^7$, three groups in addition to the ground state groups are observed. The assignment of all these additional groups to the primary reaction seems to be consistent with the group energies at the two angles of observation. The assignment then leads to an energy level scheme for Be^7 in which excited levels are located at 205, 470, and 745

kev above the ground state. The evidence is weakest for the level at 745 kev. In addition, two levels in A^{87} are confirmed in the spectrum obtained from the bombardment of LiCl. These levels fall at 1.40 and 1.65 Mev above ground.

The authors wish to acknowledge the help of Dr. H. Primarkoff who originally suggested the investigation and with whom were held many invaluable discussions. One of us (K.B.M.) acknowledges his Studentship from the Science and Industry Endowment Fund, Commonwealth of Australia. The excellent work of Miss Eileen Dennison in scanning the plates is gratefully acknowledged.

Study of the Multiple Scattering of Fast Charged Particles in a Gas and Its Role in the Interpretation of Cloud-Chamber Tracks*

GERHART GROETZINGER, MARTIN J. BERGER, AND FRED L. RIBE
Institute for Nuclear Studies, University of Chicago, Chicago, Illinois
 (Received September 19, 1949)

The curvature of the track of a fast charged particle in a magnetic cloud chamber varies along the track because of the multiple scattering of the particle by the gas in the chamber. By measurement of the mean and the fluctuations of the curvature, it is possible (1) to determine the multiple scattering in a gas of a particle of known mass, and (2) to estimate, on the basis of a verified multiple scattering law, the mass and energy of a particle. The statistical uncertainty inherent in such estimates is discussed. The multiple scattering of 132 beta-particles, ranging in energy from 50 to 1700 kev, with a total path length of 1800 cm in one atmosphere of argon, was measured and compared with the predictions of the theories of Bothe, Williams, Goudsmit and Saunderson, Molière, and Snyder and Scott. The theories of Molière, and Snyder and Scott, as well as that of Williams, if an available parameter is suitably adjusted, agree fairly well with our results.

I. INTRODUCTION

THERE is considerable experimental evidence concerning the multiple scattering of fast charged particles in foils, which in many instances does not conform very well to the various theories of multiple scattering developed by W. Bothe,¹ E. J. Williams,² S. Goudsmit and J. L. Saunderson,³ G. Molière,⁴ and H. S. Snyder and W. T. Scott.⁵ Multiple scattering in gases, however, has been little investigated so far. During the course of a cloud-chamber investigation of electron-positron pair production, L. Simons and K. Zuber⁶ have touched upon the multiple scattering of

these particles in the mixture of argon and methyl iodide with which their cloud chamber was filled, and found their results in agreement with the theory of Bothe. E. A. Luebke, G. S. Klaiber, and G. G. Baldwin⁷ examined the cloud-chamber tracks of protons in air, and L. W. Smith and P. G. Kruger⁸ those of electrons in air; their results are consistent with predictions by H. A. Bethe⁹ based on the theory of Williams, concerning the errors introduced by multiple scattering in the evaluation of cloud-chamber tracks. On the other hand, Johanna Ruling and Herma Gheri¹⁰ claim that the mean square scattering angle of electrons in air with energies from 4 to 10 Mev, as observed in a cloud chamber, is from five to fifty times greater than predicted by the theory of Williams.

The purpose of this paper is to study the multiple scattering of electrons in argon. Scattering data obtained from the cloud-chamber tracks of beta-particles will be compared with the predictions of various

* Assisted by the Joint Program of the ONR and AEC. Preliminary results of this paper have been presented at the 1948 Chicago meeting of the American Physical Society (Martin J. Berger and Gerhart Groetzinger, Phys. Rev. **75**, 342A (1949)). See also Ribe, Berger, and Groetzinger, Phys. Rev. **77**, 760 (1950).

¹ W. Bothe, *Handbuch der Physik* (Verlag Julius Springer, Berlin, 1933), Vol. 22, II, p. 1.

² E. J. Williams, Proc. Roy. Soc. **169**, 531 (1939); Phys. Rev. **58**, 292 (1940).

³ S. Goudsmit and J. L. Saunderson, Phys. Rev. **57**, 24 (1940); Phys. Rev. **58**, 36 (1940).

⁴ G. Molière, Zeits. f. Naturforsch. **3a**, 78 (1948). (This paper contains a summary of experimental results on scattering by foils.)

⁵ H. S. Snyder and W. T. Scott, Phys. Rev. **76**, 220 (1949).

⁶ L. Simons and K. Zuber, Proc. Roy. Soc. **159**, 383 (1937).

⁷ E. A. Luebke, G. S. Klaiber and G. G. Baldwin, Phys. Rev. **71**, 657 (1947).

⁸ L. W. Smith and P. G. Kruger, Phys. Rev. **72**, 357 (1948).

⁹ H. A. Bethe, Phys. Rev. **70**, 821 (1946).

¹⁰ Johanna Ruling and Herma Gheri, Acta Phys. Austriaca **2**, 335 (1948).

theories. Furthermore, the role of multiple scattering as a source of error as well as a source of information in the interpretation of cloud-chamber tracks will be discussed.

The amount of information obtainable from the shape of a cloud-chamber track depends on the magnitude of the deflection which the particles undergo under the combined influence of the magnetic field, and of the scattering by the atoms of the gas in the chamber. In the paper by Bethe, mentioned above, the influence of multiple scattering on the mass determination of the meson was investigated. Primarily interested in the tracks of fairly heavy particles, which show little deflection (i.e., tracks short compared to their radius of curvature), Bethe approximated the entire track (as projected on a plane perpendicular to the magnetic field) by a "best circle," whose radius was taken as the mean radius of curvature of the track. In an Appendix dealing with tracks long compared to their radius of curvature, he used essentially the same approximation, the only difference being a small correction due to the increased curvature.

The tracks of electrons will generally have considerable curvature. To extract the maximum amount of information, it is necessary, as already pointed out by Simons and Zuber, to utilize not only the mean curvature, but also the fluctuations of the curvature. This can be done by dividing a strongly curved track into a number of sections whose curvatures are measured separately, a procedure which adapts itself naturally to the case of tracks far from circular (e.g., with sharp bends due to single scattering). This analysis makes it possible to test, by means of a magnetic cloud chamber, the validity of a multiple scattering theory for particles of known mass and charge. Conversely one can, on the basis of a verified multiple scattering law, determine the mass and energy of a particle from the shape of its cloud-chamber track, without having recourse to other information such as that obtained from the ionization of the track.

II. RESUMÉ OF MULTIPLE SCATTERING THEORIES

The angular deflection φ , as projected on a plane containing the direction of incidence, which a particle undergoes as the result of multiple scattering upon traversing a layer of matter, is approximately distributed normally:

$$dF(\varphi) = (2\pi\sigma^2)^{-\frac{1}{2}} \exp(-\varphi^2/2\sigma^2) d\varphi + dF'(\varphi), \quad (1)$$

where the correction term $dF'(\varphi)$ (plural and single scattering tail) is important for large angles only. The variance σ^2 (mean square angular deflection) of the normal part of the distribution can be expressed as the product of two factors, say Q and G , of which Q depends on the interaction between the particle and the nuclei of the scattering atoms, while G takes into account the

structure of these atoms (screening, etc.) as well as statistical considerations.

The various theories proposed by Bothe, Williams, Goudsmit and Saunderson, and Molière, all give Q as:

$$Q = \frac{4\pi N x e^4 Z^2}{p^2 v^2}, \quad (2)$$

where p and v are the momentum and velocity of the particle; e the charge of the electron; Z the atomic number; N the number of nuclei per cm^3 ; and x the thickness of the scattering substance (in the direction of incidence).

The various theories differ in their expressions for G , as well as in the small corrections $dF'(\varphi)$.

Bothe and Williams assume that the multiple scattering deflections are the sum of many small individual deflections to which the Gaussian error law is applied. These individual spatial deflections range from a minimum θ_{min} (due to screening) up to a maximum θ_{max} , which must be introduced to keep the mean square deflection finite.

Bothe¹ effectively replaces G , which is approximately independent of the mass and energy of the scattered particle, by the numerical value:

$$G = 4.125, \quad (3a)$$

which he derives from a number of experiments on the multiple scattering of alpha- and beta-particles in foils.

According to Williams²

$$G = \log(\theta_{\text{max}}/\theta_{\text{min}}) \quad (3b)$$

or

$$G = \log(\varphi_{\text{max}}/\varphi_{\text{min}}), \quad (3c)$$

where θ_{max} and θ_{min} are spatial, φ_{max} and φ_{min} projected angles. With $\alpha = (mc/p)(Z^{\frac{1}{2}}/137)$ (m is the electronic mass) Williams proposes

$$\theta_{\text{min}} \sim \alpha \quad (4a)$$

and

$$\varphi_{\text{min}} \sim \alpha, \quad (4b)$$

and suggests furthermore that on the basis of a more refined consideration of screening

$$\varphi_{\text{min}} \sim 1.75\alpha. \quad (4c)$$

Williams points out that θ_{max} is a somewhat arbitrary quantity without a very clear-cut physical significance. It must be large enough so that angles larger than θ_{max} make only a negligible contribution to the scattering. On the other hand, it must be considerably smaller than the mean deflection σ for the path length considered, in order for the application of the Gaussian error law to be justified. Several definitions have been proposed. The definition

$$\varphi_{\text{max}} = (\frac{1}{2}Q)^{\frac{1}{2}} \quad (5a)$$

assures (according to Williams) that a particle traversing a layer of matter of thickness x will on the

average make only one collision resulting in a projected deflection greater than φ_{\max} . For particles of high momenta one can use the fact that because of the finite size of the nucleus practically no deflections will occur larger than λ/b where b is the nuclear radius and $2\pi\lambda$ the de Broglie wave-length of the scattered particle, which leads to

$$\theta_{\max} \sim \lambda/b. \quad (5b)$$

Taking $b = 0.57e^2Z^{1/3}/mc^2$ and using θ_{\min} given by Eq. (4a) gives (see reference 17)

$$G = 2 \log(181Z^{-1}). \quad (3d)$$

Bethe⁹ uses Williams theory with

$$\theta_{\min} = 0.757\alpha (= mcZ^{1/3}/181p) \quad (4d)$$

in connection with

$$\theta_{\max} = 0.1 \text{ radian}, \quad (5c)$$

which is the approximate magnitude of the smallest single scattering deflection which can be recognized as such in a cloud chamber.

Goudsmit and Saunderson³ propose

$$G = \log(150/137\alpha) \quad (3e)$$

and

$$G = \log(166/137\alpha) \quad (3f)$$

depending on whether their calculations are based on the Thomas-Fermi model or on the use of a Wentzel potential for the potential distribution in the atom.

Molière⁴ adopts a procedure, originally invented by G. Wentzel¹¹ which consists of first determining separately the contributions to the scattering distribution due to the particles scattered once, twice, \dots n times in a layer of matter, then summing these contributions to obtain the total angular scattering distribution. The improvement due to Molière is the evaluation of these angular distributions on the basis of an exact quantum-mechanical solution of the single scattering problem.

According to Molière, the angular multiple scattering distribution is again approximately normal, with G defined by

$$\frac{e^G}{(G)^{1/2}} = 1.31 \frac{Q^{1/2}}{\theta_{\min}}, \quad (3g)$$

θ_{\min} being a minimum (screening) angle defined as

$$\theta_{\min} = 1.142\alpha \left[1.13 + \left(\frac{3.76Z^2}{137^2\beta^2} \right)^{1/2} \right]. \quad (4c)$$

Molière obtains an explicit expression for the correction $dF'(\varphi)$ to the normal distribution in terms of a power series in $1/G$. Finally it must be mentioned that, in order for the approximations made in Molière's theory of multiple scattering to be justified, it is necessary to have a minimum path length such that $G \gtrsim 2.25$.

¹¹ G. Wentzel, Ann. d. Physik 69, 335 (1922).

The most recent theory of multiple scattering is that of H. S. Snyder and W. T. Scott,⁵ which is based on an exact solution and numerical integration of an integral diffusion equation. In spite of their different approach their results agree rather closely with those of Molière, so that one could again split off a Gaussian part of the distribution. (For a comparison of the two theories see Section VI.)

It is often advantageous to confine one's attention to the normal part of the distribution (a) for an experimental check of scattering theories because of the rarity of large deflections particularly in a gas, (b) when determining the properties of a particle because of the greater ease of statistical treatment. Fortunately, this is possible in cloud-chamber work, where the entire track of the particle is observable. If one excludes from consideration deflections larger than 2.8σ , the single scattering tail is practically eliminated. It turns out that the variance of this truncated distribution, computed according to Molière's complete expression (including the correction $dF'(\varphi)$) differs from σ^2 by less than 5 percent.

III. ANALYSIS OF A CLOUD-CHAMBER TRACK

Consider a cloud-chamber track, projected on a plane perpendicular to the magnetic field in the chamber, and divided into a number of sections by a set of points equidistant along the track. If these sections are sufficiently small compared to their radii of curvature, the angles between the tangents to the track at successive division points can each be considered as the sum of a constant magnetic deflection and a normally distributed multiple scattering deflection. Thus the set of angles $\varphi_1, \varphi_2, \dots, \varphi_n$ obtained from one track divided into n sections each of length x , can be considered as a sample of n values of a normal population with the distribution function

$$dF(\varphi) = (2\pi\sigma^2)^{-1/2} \exp[-(\varphi - \mu)^2/2\sigma^2] d\varphi, \quad (6)$$

where

$$\mu = x/\rho_H = xHe/pc \quad (6a)$$

is the magnetic deflection.†

This result is subject to a number of qualifications. For one thing, the multiple scattering theory as set forth in Section II assumes that all angles are projected onto a plane containing the direction of incidence. This condition is not exactly fulfilled if the track is projected onto a plane perpendicular to the magnetic field, which will in general be slightly inclined with respect to the directions of incidence for the various sections of the track. The magnitudes of these angles of inclination depend on the depth of the illuminated region of the cloud chamber (approximately between two parallel planes perpendicular to the magnetic field), and on the length of the track confined to this illuminated region. It may be added here that if the depth of the illu-

† Angular deflection \sim path length \times "curvature." For the sake of convenience in notation, we keep the discussion mainly in terms of angular deflections rather than "curvatures."

minated region is of the same order of magnitude as the section length x , there will be no limitation on the multiple scattering angle in an individual section of the track, with the possible exception of the last one or two, where the particle may be close to the boundary of the illuminated region. The error due to the projection of the track on the plane perpendicular to the magnetic field is discussed in more detail in Appendix I. It does not exceed ± 2 percent under our experimental conditions. There is an additional error (not greater than 2 percent) due to the inclination of the track with respect to the plane of projection, which makes the effective magnetic field and thus the magnetic deflection somewhat smaller than assumed in Eq. (6a). Of course both these errors can be eliminated, in the interest of accuracy, and at the expense of expediency, if all angles are measured stereoscopically.

Hitherto it has been tacitly assumed, that the energy of the particle remains constant over the entire track. In Appendix II the effect of energy loss is considered. For electrons of initial energies as low as 50 kev in argon at a pressure of one atmosphere it is found to be negligible.

The statistical information contained in the set of observed angles $\varphi_1, \varphi_2, \dots, \varphi_n$ can be summarized by means of the sample mean

$$m = \frac{1}{n} \sum_{i=1}^n \varphi_i, \tag{7}$$

the sample variance about the true mean

$$S^2 = \frac{1}{n} \sum_{i=1}^n (\varphi_i - \mu)^2, \tag{8}$$

and the sample variance about the sample mean

$$s^2 = \frac{1}{n-1} \sum_{i=1}^n (\varphi_i - m)^2. \tag{9}$$

As n increases, m approaches μ , while S^2 and s^2 approach σ^2 . If, for the sake of convenience, we introduce the auxiliary variables

$$u = (m - \mu) / \sigma n^{\frac{1}{2}}, \tag{10}$$

$$X^2 = nS^2 / \sigma^2, \tag{11}$$

$$\chi^2 = (n-1)s^2 / \sigma^2, \tag{12}$$

$$t = (m - \mu) / sn^{\frac{1}{2}}, \tag{13}$$

their distribution functions are the following standard statistical distributions:¹²

$$dF(u) = \frac{1}{(2\pi)^{\frac{1}{2}}} \exp(-u^2/2) du, \tag{10a}$$

$$dF(X^2) = \frac{(X^2/2)^{\frac{1}{2}(n-3)}}{2\Gamma(n/2)} \exp(-X^2/2) d(X^2) \tag{11a}$$

χ^2 distribution (with n degrees of freedom).

$$dF(\chi^2) = \frac{(\chi^2/2)^{\frac{1}{2}(n-4)}}{2\Gamma[(n-1)/2]} \exp(-\chi^2/2) d(\chi^2) \tag{12a}$$

χ^2 distribution (with $n-1$ degrees of freedom).

$$dF(t) = \frac{\Gamma(n/2)}{\Gamma[(n-1)/2][\Gamma(n-1)\pi]^{\frac{1}{2}}} \left(1 + \frac{t^2}{n-1}\right)^{-n/2} dt \tag{13a}$$

Student- t distribution (with $n-1$ degrees of freedom).

Integrals of the χ^2 and Student- t distributions are available in tabulated form.¹³

To test the hypothesis that the particle producing the track has a certain mass and energy, we express these quantities in terms of μ and σ^2 and compute by means of expression (10a) or (13a) the probability of obtaining a value of m exceeding the actually found sample mean m_0 , and by means of expression (11a) the corresponding probability of obtaining a value S^2 exceeding the actually found sample variance S_0^2 . Thus the test of a hypothesis can be based either on a consideration of the mean or the variance of the set of measured angles. For a given energy, the relative accuracy of the two tests depends upon the strength of the magnetic field and vice versa. Let Δm and ΔS be the standard deviations of m and S . Then it follows from (10a), (11a), (12a) and (13a) that

$$\Delta m / m \sim \sigma / n^{\frac{1}{2}} \mu, \tag{14}$$

$$\Delta S / S \sim \Delta s / s \sim 1 / (2n)^{\frac{1}{2}}, \tag{15}$$

which indicates that both tests increase in accuracy with increasing n , that the test of the mean increases in accuracy with increasing magnetic field (which is proportional to μ) and that the test of the variance is more accurate than the test of the mean, if $\sigma/\mu > 1/\sqrt{2}$. For instance, for electrons with an energy of 1.5 Mev in a cloud chamber filled with argon at a pressure of 1 atmos., the test of the mean is more accurate for magnetic field strengths above, that of the variance for field strengths below 300 gauss.

A remark may be in order concerning the use of the Student- t distribution to test a hypothesis. It is seen that expression (13a) does not contain the theoretical variance σ^2 ; therefore this test is based merely on the normal form of the angular distribution of multiple scattering deflections, but does not demand a knowledge of the theoretical mean square angle of deflection.

The best estimates of μ and σ^2 are m_0 and s_0^2 . The

¹² See H. Cramer, *Mathematical Methods of Statistics* (Princeton University Press, Princeton, 1946).

¹³ R. A. Fisher and F. Yates, *Statistical Tables* (Oliver and Boyd, London, 1948).

standard deviations of these estimates have already been given (Eq. (14) and Eq. (15)). The best estimate of a function $F(\mu, \sigma)$ is $F(m, s)$ with a standard deviation

$$\Delta F = \{(\partial F/\partial \mu)_{\mu=m}^2(\Delta m)^2 + (\partial F/\partial \sigma)_{\sigma=s}^2(\Delta S)^2\}^{1/2}. \quad (16)$$

IV. MASS DETERMINATION

The mass of a particle can be estimated in a straightforward fashion from the sample mean and variance of the observed angular deflections of its track with a standard deviation (calculated according to Eq. (16)), proportional to $[1 - v^2/c^2]^{-1/2}$ so that for high velocities the statistical error can become considerable.

The mass of a particle can also be estimated by comparing its scattering with that of a particle of approximately the same momentum and known properties, or preferably with the scattering of a group of such particles, an estimate which is nearly independent of the controversial factor G of the scattering law (Eqs. (3a) to (3g)) and of exact knowledge of the experimental conditions, such as the composition of the scattering gas, the magnetic field, etc.

Suppose we have two tracks of n_a and n_b sections, respectively, produced by two particles of the same momentum, but different masses, M_a and M_b . Let s_a^2 and s_b^2 be the observed sample variances, and σ_a^2 and σ_b^2 the theoretical variances of the respective normal multiple scattering distributions. If the momenta, i.e., the means of these distributions, are known to be equal, the ratio of the sample variances is distributed according to the Fisher- z distribution $dF(z)$ (see reference 12). Let

$$z = \frac{1}{2} \log \{ (n_a - 1)n_a s_a^2 / (n_b - 1)n_b s_b^2 \}. \quad (17)$$

Then

$$dF(z) = \frac{\text{const. } e^{(n_a - 1)z}}{\{(n_a - 1)e^{2z}/\sigma_a^2 + (n_b - 1)/\sigma_b^2\}^{1/2} (n_a + n_b - 2)}. \quad (17a)$$

Under ordinary circumstances, however, the determination of the momenta will be made from the cloud-chamber tracks and thus be subject to a statistical error, which may amount to 5 percent or more. In this case it is preferable to compare for the two tracks the ratios of their magnetic to their multiple scattering deflections. These ratios, which are proportional to the velocities of the two particles, are rather insensitive to errors in the momentum. Let

$$l_{ab} = (m_a/s_a)/(m_b/s_b) \quad (18a)$$

and

$$\lambda_{ab} = (\mu_a/\sigma_a)/(\mu_b/\sigma_b). \quad (18b)$$

Then it can be shown (see Appendix III), that the variable

$$U = \left(1 - \frac{l_{ab}}{\lambda_{ab}}\right) \times \left\{ \frac{(1/n_a)(\sigma_a/\mu_a)^2 + 1}{2(n_a - 1)} + \frac{1/n_b + 1/\lambda_{ab}^2}{2(n_b - 1)} l_{ab}^2 \right\}^{-1/2} \quad (18c)$$

TABLE I. Theoretical (after Molière) root mean square multiple scattering deflections $\sigma_1, \sigma_3, \sigma_{10}$ (in degrees for particles of mass $M=1, 3$, and 10 electron masses, and the corresponding ratios $\lambda_{1,3}$ and $\lambda_{1,10}$

$$\lambda_{1,3} = [(\sigma_3^2 + 0.1)/(\sigma_1^2 + 0.1)]^{1/2}, \lambda_{1,10} = [(\sigma_{10}^2 + 0.1)/(\sigma_1^2 + 0.1)]^{1/2}.$$

$H\rho$ Gauss cm	σ_1 deg.	σ_3 deg.	σ_{10} deg.	$\lambda_{1,3}$	$\lambda_{1,10}$
7500	2.69	3.34	8.35	1.25	3.08
10000	1.99	2.27	4.64	1.14	2.31
12500	1.58	1.73	3.53	1.10	2.20
15000	1.31	1.40	2.22	1.07	1.76
17500	1.12		1.72		1.51
20000	0.98		1.39		1.39
22500	0.87		1.16		1.30
25000	0.78		1.00		1.24

is distributed normally:

$$dF(U) = \frac{1}{(2\pi)^{1/2}} \exp(-U^2/2) dU. \quad (18d)$$

In practice it will often occur that one is comparing one unknown particle with a large group of known particles. In this case one can effectively set $n_b = \infty$. Furthermore, the term $(1/n_a)(\sigma_a/\mu_a)^2$ of Eq. (18c) will often be much less than unity if the magnetic curvature is large enough, and can then be neglected.

Scattering analysis as a means of mass determination is especially suitable for particles of small mass. Recently there have been reports in the literature of particles occurring in the cosmic radiation with masses from three to ten times that of the electron.¹⁴ As an application of the foregoing theory the distribution function $dF(U)$ was used to calculate how well such particles could be distinguished from electrons by their scattering. It was assumed that the tracks are observed

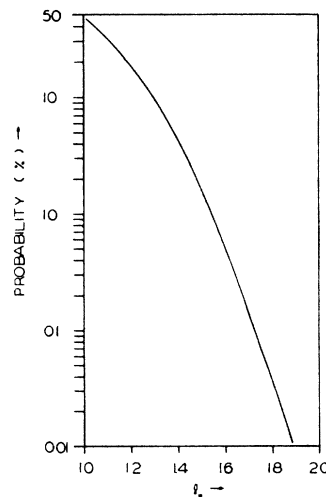


Fig. 1. Statistical fluctuations of the multiple scattering of identical particles: Probability $P_\lambda(l \geq l_0)$ calculated from Eqs. (18c) and (18d) with $\lambda=1, n_a=10, n_b=\infty$, and $(1/n_a)(\sigma_a/\mu_a)^2 \ll 1$.

¹⁴ Cf. L. Janossy and C. B. A. McClusker, Nature 163, 181 (1949).

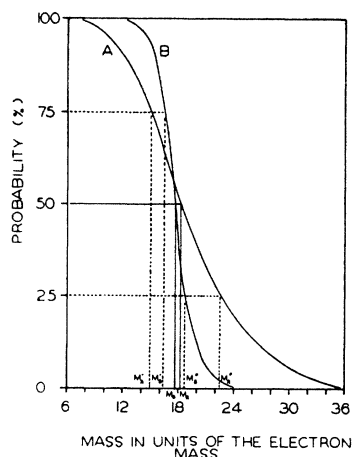


FIG. 2. Mass discrimination on the basis of multiple scattering: Probability $P_\lambda(l \geq l_0)$ calculated from Eqs. (18c) and (18d) with $l_0=2$, $\lambda=\lambda(M)$, $n_b=\infty$, $n_a=10$ (curve A), $n_a=100$ (curve B).

in a cloud chamber filled with argon at a pressure of one atmosphere, and that they are divided into sections 2 cm long. One track of an unknown particle, consisting of ten sections, is being compared with many electron tracks of the same momentum. ($n_a=10$, $n_b=\infty$).

Table I gives, for various momenta, the theoretical root mean square multiple scattering deflections σ_1 , σ_3 , σ_{10} (in degrees) for particles of mass $M=1$, 3, and 10 (in terms of electron mass) calculated according to the theory of Molière as well as the corresponding ratios

$$\lambda_{1,3} = (\mu_1/\sigma_1)/(\mu_3/\sigma_3) = \sigma_3/\sigma_1,$$

and

$$\lambda_{1,10} = (\mu_1/\sigma_1)/(\mu_{10}/\sigma_{10}) = \sigma_{10}/\sigma_1.$$

(Here $\mu_1=\mu_3=\mu_{10}$.) These ratios are more likely to be correct than σ_1 , σ_3 , and σ_{10} because they do not, as pointed out before, depend very much on the factor G of the theoretical variance, which differs for the various theories of multiple scattering. In order to account for the experimental error in measuring the angles of deflection, an "experimental error variance" of $(0.3^\circ)^2$ was added to σ_1^2 , σ_3^2 , and σ_{10}^2 before the ratios $\lambda_{1,3}$ and $\lambda_{1,10}$ were computed. This value was arrived at by an experimental investigation of the accuracy of measurement to be described later.

Consider the case where the track of the unknown particle is being compared with those of test particles of approximately the same momentum, the ratio l being found experimentally to have the value l_0 . Disregarding statistical fluctuations, one would assume that the mass of the unknown particle is such that $\lambda=l_0$. However, in view of the fluctuations, one may test the hypothesis that the unknown particle actually has the same mass as the test particle(s) ($\lambda=1$). In Fig. 1 is plotted, on the hypothesis that $\lambda=1$, the probability $P_\lambda(l \geq l_0)$ of obtaining an l greater than or equal to the observed l_0 , assuming one "unknown" track of

10 sections and a large number of test particles (electrons). The ordinates corresponding to values of the abscissa $l_0=\lambda_{1,3}$ and $l_0=\lambda_{1,10}$ are then a measure of the likelihood that particles of apparent mass three and ten, respectively, have in reality mass one, $\lambda_{1,3}$ and $\lambda_{1,10}$ become small enough to make this probability appreciable (25 percent) for momenta higher than $H\rho=10,000$ and $H\rho=25,000$ Gauss-cm, respectively.

Next we consider the use of Eqs. (18c, d) to make a mass estimate. As an example, Fig. 2 describes the hypothetical case of an unknown particle of measured $H\rho=1.7 \times 10^4$ Gauss-cm which scatters twice as much as electrons of the same momentum with which it is being compared ($l_0=2$). To each assumed mass M (in units of the electron mass) for the unknown particle there corresponds a $\lambda(M)$ and a probability $P_\lambda(l \geq l_0)$ of obtaining an $l \geq l_0=2$. These probabilities are plotted against different values of M . Curve A refers to the case in which one track, curve B to the case in which a group of 10 tracks of particles (known to be identical) is being compared with a large group of electron tracks.

The best estimates of the mass in these two cases are the values corresponding to the probability level of 50 percent (M_A and M_B , respectively, shown in Fig. 2). \ddagger The values of the mass corresponding to the 25 percent and 75 percent levels of probability M_A' , M_B' and M_A'' , M_B'' , respectively, are the limits of the "50 percent confidence interval" of the mass estimates. \S

In the interest of accuracy, especially for particles of high energy, it is desirable to have the mean multiple scattering angle as large as possible. This angle is proportional to $Z(A)^{\frac{1}{2}}$ where Z is the atomic number and A the pressure in atmospheres of the scattering gas. Chambers operating at pressures between 100 and 200 atmospheres have recently been described in the literature. 15 It appears possible, by an examination of multiple scattering in such high pressure chambers, to distinguish between mesons of approximately 200 and 300 electron masses, if their energies do not exceed 50 Mev.

TABLE II. Minimum path length in argon (1 atm., 25°C).

v/c	$x_{\min}(\text{cm})$	v/c	$x_{\min}(\text{cm})$
0.5	0.46	0.9	1.33
0.6	0.63	0.95	1.47
0.7	0.83	0.97	1.54
0.8	1.04	1.00	1.61

\ddagger M_A differs slightly from M_B due to the fact that the distribution is based on an approximation (see Appendix III).

\S The limits of the "50 percent confidence interval" are roughly analogous to the limits of the probable error. For an exact definition see, for instance, M. G. Kendall, *The Advanced Theory of Statistics* (Charles Griffin and Company, Ltd., London, 1948), Vol. II, p. 62.

15 R. Richard-Foy, see L. Le Prince-Ringuet, *Les Rayons Cosmiques* (Michel, Paris, 1945); G. E. Valley and J. A. Vitale, *Phys. Rev.* **75**, 1328A (1949); Shutt, Hoke, Tuttle, and Neil, *Phys. Rev.* **75**, 1329A (1949).

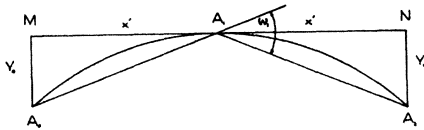


FIG. 3. Geometrical analysis of a cloud-chamber track used in determining multiple scattering.

V. EXPERIMENTAL PROCEDURE

The cloud-chamber tracks of 132 beta-particles from a P^{32} source,^{||} ranging in energy from approximately 50 to 1700 kev, were examined. The minimum length of the tracks was 12 cm, the average length 14 cm. They were obtained in a horizontal cloud chamber with a diameter of 24 cm, and an illuminated region 2.5 cm deep, filled with argon at a pressure of one atmosphere at 25°C. The source was mounted about 4 cm from the rim of the chamber in the center of the illuminated region. The magnetic field was produced by a set of Helmholtz coils and ranged from 330 to 355 gauss for different exposures.

Table II gives the minimum path length in one atmosphere of argon which will make the quantity G in Molière's theory larger than 2.25 (condition of applicability of multiple scattering theory). For our experiment we adopted a path-length of approximately 2 cm (i.e., the tracks were divided into 2-cm sections) which satisfied Molière's condition for electrons of all energies. It was this theoretical consideration rather than the difficulty of measurement which put a lower limit on the size of the sections.

Instead of the angles φ_i between the tangents to the projected track at the division points, we preferred to measure the angles ω_i between successive chords connecting these points. (See Fig. 3 in which the curvature is exaggerated.) By an extension of an argument of S. Lattimore¹⁶ to the case of multiple scattering in the

presence of a magnetic field it will be shown that the information provided by the angles ω_i is equivalent to that provided by the angles φ_i , except that the number of ω_i 's is one less than the number of φ_i 's. Figure 3 shows part of a cloud-chamber track, projected on a plane perpendicular to the magnetic field, and passing through the points A_0 , A_1 , and A_2 . The line (NA_1M) is tangent to the track at A_1 . It is seen from the figure that the angle between (A_0A_1) and (A_1A_2)

$$\omega_1 = y_0/x' + y_1/x'. \quad (19)$$

It can be shown¹⁷ that the lateral deflections y_0 and y_1 , each are distributed normally, with mean $x'\mu/2 = x'^2/2\rho_H$ ($\rho_H = pc/He$) caused by magnetic deflection, and variance $\sigma_y^2 = \frac{1}{3}x'^2\sigma^2$ due to multiple scattering, where σ^2 is the theoretical mean square angular scattering deflection. Because of the presence of the magnetic field, the distance x' does not correspond exactly to the distance x (thickness of matter traversed) as understood in the theory of multiple scattering. If the total angle subtended by the section of the track considered does not exceed 15°, the chord length (A_iA_{i+1}) will differ at most by 3.5 percent from x' , and 0.3 percent from the arclength $[A_iA_{i+1}]$. The length x is larger than x' but smaller than the arc length. The procedure adopted was to make all chords of equal length (2 cm) and consider them equal to x . The mean scattering angle is proportional to the square root of x and will thus be off by at most 1.75 percent. ω_1 is the sum of two normally distributed quantities and is therefore itself normally distributed; this is also true of $\omega_2 = (y_1 + y_2)/x'$, ..., $\omega_n = (y_{n-1} + y_n)/x'$. The multivariate distribution function of the angles ω_i is:

$$dF(\omega_1, \omega_2, \dots, \omega_n) = \text{const.} \exp \left[-\frac{3}{4\sigma^2} \sum_{i=1}^n (\omega_i - \mu)^2 \right] d\omega_1 \dots d\omega_n. \quad (20)$$

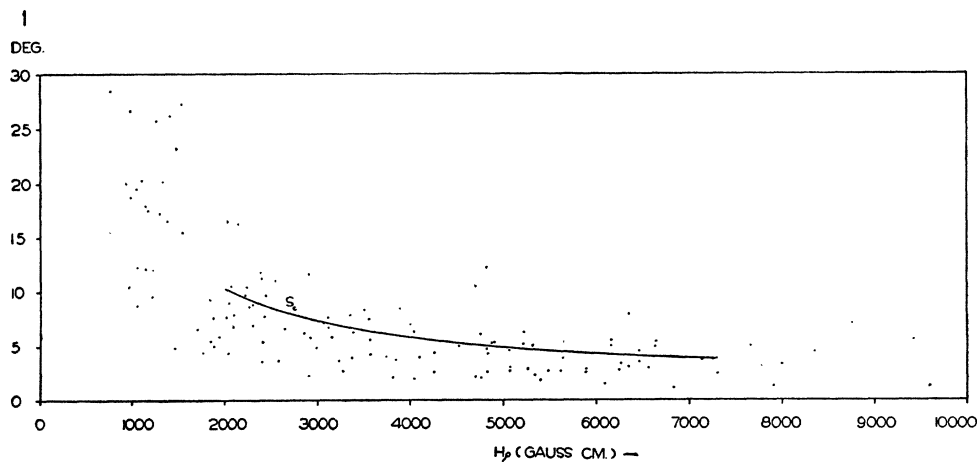


FIG. 4. Multiple scattering of electrons in one atmosphere of argon at 25°C: r.m.s. angular scattering deflection in degrees for 2-cm path length plotted against measured H_p .

^{||} The radioactive P^{32} was supplied by the Isotope Branch of the AEC, Oak Ridge, Tennessee.

¹⁶ S. Lattimore, *Nature* **161**, 518 (1948).

¹⁷ B. Rossi and K. Greisen, *Rev. Mod. Phys.* **13**, 240 (1941).

Again, as in Section III, we form the sample mean

$$\bar{\omega} = \frac{1}{n} \sum_{i=1}^n \omega_i \quad (21)$$

and the sample variances,

$$(\Omega^2)_{Av} = \frac{1}{n} \sum_{i=1}^n (\omega_i - \mu)^2 \quad (22)$$

and

$$(\omega^2)_{Av} = \frac{1}{n-1} \sum_{i=1}^n (\omega_i - \bar{\omega})^2. \quad (23)$$

As n increases, $\bar{\omega}$ approaches μ , while $(\Omega^2)_{Av}$ and $(\omega^2)_{Av}$ approach $2/3\sigma^2$. The sample mean, in terms of the y 's (Fig. 3), can be written

$$\bar{\omega} = (1/nx')(y_0 + 2y_1 + \cdots + 2y_{n-1} + y_n). \quad (24)$$

It is distributed normally with mean μ and variance $(4n-2)\sigma^2/3n^2$. The sample variance $(\Omega^2)_{Av}$ is a quadratic form in $n+1$ independent uncorrelated variables y_0, y_1, \cdots, y_n , which by a coordinate transformation can be reduced to the sum of the squares of n independent quantities (this number is n rather than $n+1$, because there are only n independent measurements $\omega_1, \omega_2, \cdots, \omega_n$). This transformation will at the same time reduce the exponent of the distribution function (20) to a sum of squares. $3(n-1)(\Omega^2)_{Av}/2\sigma^2$ is then distributed χ^2 with n degrees of freedom (see Eq. (11a), Section III). Similarly it can be shown that $3n(\omega^2)_{Av}/2\sigma^2$ is distributed χ^2 with $n-1$ degrees of freedom, and $(\bar{\omega} - \mu)/[(\omega^2)_{Av}]^{1/2}$ according to the Student- t distribution with $(n-1)$ degrees of freedom.

The angles between successive chords were measured as follows: The image of the track on the 35-mm photographic negative was projected on a sheet of drawing paper with an enlargement giving the original size of the track, and 2-cm sections were then laid off along the image of the track by dividers. The sheet containing the set of division points was mounted on a drafting table, the points were connected by straight lines representing the chords, and the angles between successive chords were measured by means of a drafting machine.

The experimental error due to optical distortions, emulsion distortion, and inaccuracy of angular measurement was estimated as follows: circular arcs of radii 5, 10, 15, and 25 cm were drawn on a sheet of drawing paper and photographed in various orientations in a horizontal plane in the position of the sensitive portion of the cloud chamber, using the same optical arrangement employed originally to photograph the tracks. Each circle was then measured independently by three observers, in the same manner as the cloud-chamber tracks. The resulting error, the apparent root mean square angular scattering deflection, was averaged for all observers for each radius, and found to be almost independent of the radius. The average angle was 1.05° .

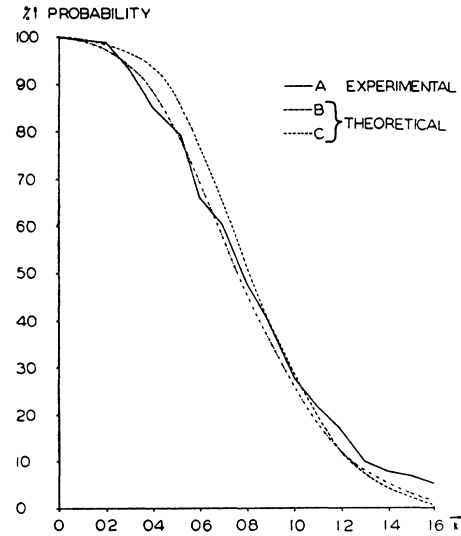


FIG. 5. Statistical fluctuations of multiple scattering: Curve A (experimental): Fraction of tracks from Fig. 4 with $s = ks_L.sq.$ plotted against k . Curves B and C (theoretical): Integrals of χ^2 distributions of $n-1$ degrees of freedom, respectively, between the limits of nk^2 and ∞ , plotted against k (with $n=6$, and $n=5$, respectively).

In a separate investigation concerning the accuracy which can be obtained in measuring angular deflections, the same circular arcs were also measured directly on the films by means of a microscope with a mechanical stage, adapted for accurate angular measurements, the magnification used being 51. It was found that this method, while more laborious, will make the experimental error less than 0.3° .

The error due to the turbulence in the chamber is negligible. A few high energy cosmic-ray meson tracks which occurred incidentally in the course of the experiment were investigated. They appeared to be slightly curved. By measuring the deviation from a straight line an upper limit of the spurious curvature due to turbulence can be determined. The deviation was measured by means of a micrometer arrangement at points along the track 1 cm apart, and a circle was fitted to the resulting plot of these deviations. The smallest radius of curvature so obtained was larger than 250 cm which corresponds to a negligible error not exceeding 0.3° per 2-cm section.

VI. EXPERIMENTAL RESULTS

The experimental results are shown in Fig. 4, in which the individual root mean square multiple scattering deflections $s = (\frac{2}{3})^{1/2} [(\omega^2)_{Av}]^{1/2}$ are plotted against $H\rho$, each of the 132 points representing one track. 90 percent of these tracks have 6 to 8 sections, the rest 9 to 13. 100 points corresponding to apparent momenta above $H\rho = 2000$ Gauss-cm were fitted to a smooth curve by the method of least squares. The lower limit for the momenta was chosen so as to avoid unduly large errors resulting from our only approximately correct manner

of projecting and measuring the tracks. σ^2 can be approximated very well by a second-degree polynomial in $1/(H\rho)^2$. Therefore the least-square curve was obtained by fitting the experimental mean square angles s^2 to such a polynomial, which was found to be:

$$s_{L.SQ.}^2 = 4.307 + 3.897 \times 10^8 (H\rho)^{-2} - 2.294 \times 10^{14} (H\rho)^{-4}. \quad (25)$$

The probable error in $s_{L.SQ.}^2$, calculated from the sum of the residues in least square fitting, was found to be 10 percent.

The least-square fitting had to be carried out as if the momenta for each track were accurately known. The actual statistical uncertainty in $H\rho$ has two effects. Regardless of whether the error in $H\rho$ is negative or positive, it tends to cause an under-estimate of the scattering, since the mean radii (or mean deflections) are calculated in a way which automatically minimizes the mean scattering angles. (See Eq. (22).) This effect has already been accounted for by the use of the sample variance s^2 about the sample mean, which is larger than the sample variance S^2 about the true mean, by a factor $n/(n-1)$. Secondly the uncertainty in $H\rho$ will itself directly affect the shape of the least-square curve. It can be reasonably assumed, however, that with the error in $1/(H\rho)$ equally likely to be positive or negative, the net effect will be insignificant when we are dealing with a large number of particles, in view of the fact that s is very nearly a linear function of $1/(H\rho)$ (see Eq. (25)), where the quadratic term in $(1/H\rho)^2$ is small compared to the linear term.

As mentioned before, the random experimental error due to optics, photography and personal error in measurement, will introduce a spurious root mean square deflection $s_E = 1.05^\circ$. On the assumption that the multiple scattering deflections and the "error deflection" s_E are statistically independent one can set the corrected root mean square deflection

$$s_c = (s_{L.SQ.}^2 - s_E^2)^{\frac{1}{2}}. \quad (26)$$

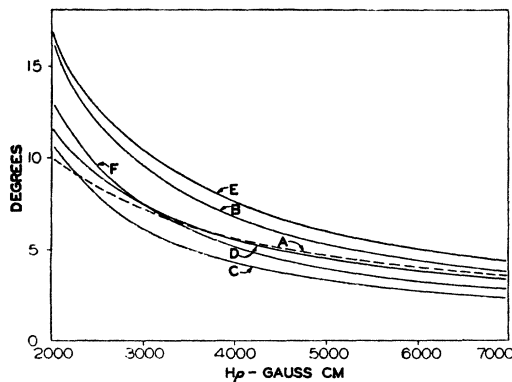


FIG. 6. Comparison of experimental results with various theories of multiple scattering. Curve A: Experimental; Curve B: Bothe; Curve C: Williams ($\varphi_{\max} = (\frac{1}{2}Q)^{\frac{1}{2}}$, $\varphi_{\min} = (mc/p) \cdot (Z^{\frac{1}{2}}/137)$); Curve D: Williams-Bethe ($\theta_{\max} = 0.1$ radian, $\theta_{\min} = (mc/p) \cdot (Z^{\frac{1}{2}}/181)$); Curve E: Goudsmit and Saunderson (Thomas-Fermi potential); Curve F: Molière.

This correction was applied to the least-square curve. The result is indicated by the solid curve of Fig. 4, which shows s_c as a function of $H\rho$. The curve was broken off at $H\rho = 7300$ Gauss-cm, which corresponds to the upper limit of the P^{32} beta-spectrum. Actually there are a few points with an apparently higher $H\rho$ (due to statistical fluctuations) which were included in the fitting of the curve.

Finally, it must be mentioned that sections of track, over which the multiple scattering deflection was more than 2.8 times larger than s for the given momentum, as well as sections with a noticeable single deflection (>0.1 rad.) were excluded from consideration, in order to vouchsafe the Gaussian form of the angular scattering distribution. In fact this exclusion came about almost automatically, since such large deflections were quite rare, and moreover tended to make the track ill-defined and difficult, if not impossible, to measure at the position where they occurred.

The dispersion of the experimental points about the "least squares" curve $s_{L.SQ.}$ (Eq. (25)) is indicated in Fig. 5. To each experimental point, with a certain value of apparent $H\rho$ and a root mean square scattering angle, s , there corresponds for the same $H\rho$ a point $s_{L.SQ.}$ on the "least squares" curve. For every number $k \geq 0$, there is a certain fraction of points such that $s \geq k s_{L.SQ.}$. This fraction is plotted for the 100 points above $H\rho = 2000$ Gauss-cm, as a function of k (curve A). Theoretically this fraction is given by the integral of the χ^2 distribution of $(n-1)$ degrees of freedom from nk^2 to ∞ , where n is the average number of angles ω_i per track. (See Eqs. (9), (12a), and (23).) For the tracks considered here this number was between five and six. Therefore the integrated χ^2 -distributions of four and five degrees of freedom are also plotted in Fig. 5 as functions of k (curves B and C). It is seen that for most values of k , the experimental curve falls well between the two theoretical curves, which confirms that

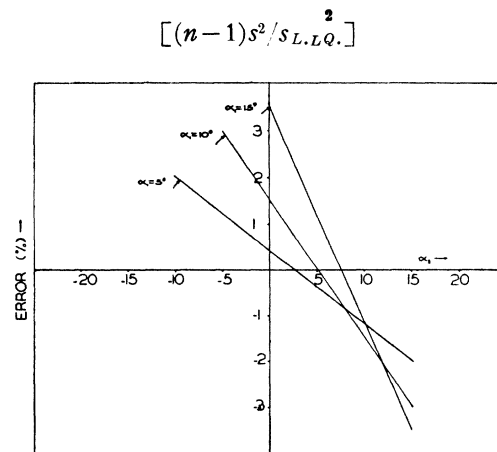


FIG. 7. Error arising from projection of cloud-chamber track section on a plane which does not contain the direction of incidence.

is distributed χ^2 , and indirectly that the angular scattering is distributed normally. Only for values of $k \gtrsim 1.3$ is the experimental frequency somewhat too high, which may indicate the presence of a small single-scattering tail.

In Fig. 6 the experimental r.m.s. angle s_c (of the normal part of the multiple scattering distribution) is compared with the corresponding angle σ as given by the various theories. The probable error in s_c is 10 percent and possibly somewhat larger at higher momenta.

The dashed curve *A* gives our experimental results (s_c). Curve *B* refers to the theory of Bothe¹ which uses a constant G (Eq. (3a)), curve *C* to the theory of Williams² with a G given by Eq. (3c), and limiting angles given in Eqs. (4b) and (5a), curve *D* to the same theory with limiting angles due to Bethe⁹ (Eqs. (3b), (4d), and (5c)), curve *E* to the theory of Goudsmit and Saunderson³ with a G given in Eq. (3e) (based on the Fermi-Thomas potential), and curve *F* to the theory of Molière.⁴ It can be seen that our experimental curve agrees best with the theory of Williams with the limiting angles due to Bethe, and with Molière's theory. The theories of Goudsmit and Saunderson and of Bothe overestimate the multiple scattering throughout the investigated momentum range. In the case of Bothe this may be due to the fact that he obtained the value 4.125 for G from experiments of multiple scattering by foils, which inadvertently may have included a certain amount of single and plural scattering. Numerical results of the theory of Snyder and Scott⁵ are not available for our experimental conditions.

According to Snyder and Scott the angular multiple scattering distribution is a function of a parameter z , which is the thickness of the scattering substance in units of the mean free path of the scattered particle. Except for a small difference due to a different expression for the energy dependence of the screening, Molière's theory could also be expressed in terms of this parameter. A comparison of the two theories was made for the smallest z ($=100$) for which numerical results are given by Snyder and Scott. This corresponds e.g., to the following conditions for electrons in one atmosphere of argon and 20°C.

Kinetic energy	Path length in cm
mc ²	3.42
2mc ²	4.05
3mc ²	4.28
4mc ²	4.37

If the projected angular deflections are expressed in units of $(2GQ)^{\frac{1}{2}}$, it turns out that for angles smaller than 0.5 the complete Molière distribution is larger than the Snyder and Scott distribution by not more than 1 percent. For angles between five and three degrees it is smaller, the maximum discrepancy being 9 percent at an angle of 1.9°. If both distributions are cut off at an angle 1.6° (which is 2.8 times the root mean square of the Gaussian part of the Molière distribution) the root

mean square angle of Snyder and Scott is about 2 percent larger than Molière's.

We are indebted to Mr. Watts Humphrey, Jr., and to Mr. Lewis Leder for their valuable help in operating the cloud chamber, measuring the tracks, and performing calculations.

Note added in proof: Our treatment in the text does not do full justice to the theory of Goudsmit and Saunderson. Equations (3e) and (3f) (also quoted by W. T. Scott, Phys. Rev. **76**, 212 (1949)) involve the assumption that $\theta_{\max} = \pi$ (all individual scattering angles regardless of magnitude are considered). As Goudsmit and Saunderson point out, it is necessary to introduce a $\theta_{\max} \ll \pi$ in order to obtain the normal approximation to the angular multiple scattering distribution. If this had been done, their theory would have been found to be in much better accord with the experimental results.

APPENDIX I: THE PROJECTION OF THE TRACK

Suppose that the magnetic field is directed along the z axis of a cartesian coordinate system. Let u_1 and u_2 be unit vectors, representing the directions of the track at the beginning and the end of the section, inclined at angles α_1 and α_2 , respectively, with respect to the $(x-y)$ plane, which is the plane of projection. Let φ be the angle between u_1 and u_2 as projected on the $(x-y)$ plane, and φ' the same angle as projected on a plane containing u_1 , which is obtained by rotating the $(x-y)$ plane about an axis perpendicular both to u_1 and the z axis.* It can be easily shown that

$$\tan \varphi / \tan \varphi' = \cos \alpha_1 \{1 + \tan \alpha_1 \tan \alpha_2 / \cos \varphi\}. \quad (27)$$

In Fig. 7 the percentage error in the projected angle is given for values of α_1 and α_2 up to 15° (valid for values of φ ranging from 0° to 20°). All of these angles are larger than those which actually occurred in our experiment. The ratio $\tan \varphi / \tan \varphi'$ can either be positive or negative and is almost independent of φ , if φ is small. In this connection it must be pointed out that the error in projection arises only in the part of the angular deflection due to scattering.

APPENDIX II: ENERGY LOSS

Let the track (projected on the plane perpendicular to the magnetic field) be divided into n sections of equal length by means of division points $P_0(a_0), P_1(a_1), \dots, P_n(a_n)$, where a is the arc-length of the track measured from its beginning. The angles $\varphi_1, \varphi_2, \dots, \varphi_n$, between tangents to the track at successive division points can again be expressed as the sum of a magnetic and multiple scattering deflection. If we consider energy loss, the magnetic deflection and the variance of the multiple scattering deflections, which are functions of the energy, will differ from section to section of the track. The magnetic deflection μ_i in the i th section (bounded by points $P_{i-1}(a_{i-1})$ and $P_i(a_i)$) can be found directly from the theory of energy loss by collision. The scattering variance in the i th section, can be expressed as follows according to Molière, who showed that in order to consider energy loss, his theory must be modified by redefining the variable Q and the screening angle θ_{\min} : For the i th section let

$$Q_i = \int_{a_{i-1}}^{a_i} q(a) da \quad (28)$$

and

$$Q_i \log \langle \theta_{i(\min)}^2 \rangle_{\mathcal{A}_i} = \int_{a_{i-1}}^{a_i} q(a) \log \theta_{\min}^2(a) da, \quad (29)$$

where

$$q(a) = \frac{4\pi NZ^2 e^4}{p^2(a) v^2(a)}, \quad (30a)$$

* This happens to be the plane containing u_1 , which has the smallest inclination with respect to the $(x-y)$ plane. According to the theory of multiple scattering, this special choice does not affect the distribution of the projected angles.

$$\theta_{\min}(a) = \frac{Z^4}{120} \frac{mc}{p(a)} \left(1.13 + \frac{3.76Z^2}{137^2 \beta^2(a)} \right)^{\frac{1}{2}} \quad (30b)$$

In (28) and (29), $g(a)$ and $\theta_{\min}(a)$ must be expressed as functions of the position along the track according to the theory of energy loss by collision. In terms of these definitions

$$e^{\sigma_i/(G_i)} = 1.31(Q_i)^{\frac{1}{2}}(\theta_{i(\min)})^{1/2}, \quad (31a)$$

$$\sigma_i^2 = Q_i G_i \quad (31b)$$

and

$$dF(\varphi_i) = (2\pi\sigma_i^2)^{-\frac{1}{2}} \exp\left[-\frac{1}{2}(\varphi_i - \mu_i)^2/\sigma_i^2\right] d\varphi_i \quad (31c)$$

Define m_1, m_2, \dots, m_n and s_1, s_2, \dots, s_n by the equations

$$\frac{1}{n} \sum_{i=1}^n \frac{\varphi_i - m_i}{s_i} = 0, \quad (32)$$

$$\frac{1}{n-1} \sum_{i=1}^n \left(\frac{\varphi_i - m_i}{s_i} \right)^2 = 1 \quad (33)$$

and by the further condition that the same relations obtain between the m_i and s_i as those which connect the μ_i and σ_i according to the theory of energy loss by collisions and the theory of multiple scattering. These m_i and s_i are the best estimates of μ_i and σ_i , with an accuracy increasing with n . They can be determined, from the conditions defining them in terms of the measured angles φ_i , and in this way the experimental scattering s_i can be expressed as a function of the experimental (apparent) magnetic deflection m_i over the range of energies represented in the track.

If one neglects energy loss and sets all $m_i = m$ (constant), $s_i = s$ (constant), then from (32)

$$\frac{1}{n} \sum_{i=1}^n \varphi_i = m$$

and from (33)

$$\frac{1}{n-1} \sum_{i=1}^n (\varphi_i - m)^2 = s^2.$$

The error thus made is measured by the ratio $R = s/s_i$ between s and the s_i corresponding to the $m_i \approx m$. R is a function of the φ_i , whose distribution function can be determined in terms of those of the φ_i , i.e., the $dF(\varphi_i)$. For electrons with an initial energy of 50 keV and a path length of 14 cm in one atmosphere of argon R_{av} was estimated to differ from unity by less than 1 percent.

APPENDIX III: DERIVATION OF EQ. (18c)

Let m and s be the sample mean and variance, μ and σ the true mean and variance of a normal variable. It was shown by N. L. Johnson and B. L. Welch¹⁸ that the ratio $m\sigma^2/s$ is distributed approximately normally with mean $(n)^{\frac{1}{2}}\mu/\sigma$ and variance

$$\frac{1 + (n\mu^2/\sigma^2)^{\frac{1}{2}}}{2(n-1)^{\frac{1}{2}}}$$

where n is the size of the sample. According to R. C. Geary¹⁹ the ratio v of the two independent normal variables has the distribution function

$$dF(v) = \frac{1}{(2\pi)^{\frac{1}{2}}} \frac{\mu_2\sigma_1^2 + \mu_1\sigma_2^2 v}{(\sigma_1^2 + \sigma_2^2 v^2)^{\frac{1}{2}}} \exp\left\{-\frac{1}{2} \frac{(\mu_1 - \mu_2 v)^2}{\sigma_1^2 + \sigma_2^2 v^2}\right\} dv \quad (34)$$

so that

$$\frac{\mu_1 - \mu_2 v}{(\sigma_1^2 + \sigma_2^2 v^2)^{\frac{1}{2}}}$$

is distributed with mean zero and unit variance, where μ_1 and σ_1 are the mean and variance of the first variable, μ_2 and σ_2 those of the second.

When considering the ratio $(m_a/s_a)(m_b/s_b)$ one can obviously combine the two results quoted above, and obtain Eq. (18c).

¹⁸ N. L. Johnson and B. L. Welch, *Biometrika* **31**, 362 (1940).

¹⁹ R. C. Geary, *JRSS* **93**, 447 (1930).

Star Fragments in Oxygen and Helium under Bombardment by 90-Mev Neutrons

JAMES TRACY AND WILSON M. POWELL
Radiation Laboratory, University of California, Berkeley, California
(Received October 17, 1949)

A study has been made of eighty-two stars produced in a mixture of oxygen and helium when a cloud chamber filled with these gases and placed in a magnetic field of 13,000 gauss was bombarded by 90-Mev neutrons. Stars having up to five prongs were observed.

Of the forty-eight 2-prong stars, 14 could be reasonably assigned to oxygen and 14 to helium. The remaining 20 were unidentified.

VERY soon after the 184-inch cyclotron¹ began to operate, a cloud chamber was placed in the beam of high energy neutrons² that was produced when the 195-Mev deuterons struck a target in the cyclotron tank. These neutrons were observed to produce stars in the gas of the cloud chamber. In individual cases it was always difficult to tell what nucleus was disintegrating. Since oxygen is always present in the cloud-chamber vapor, it was considered profitable to under-

take a detailed study of the characteristics of oxygen stars in the hope that they might be distinguished from other stars in future studies.

It was found possible to make plausible identifications of all the fragments from only 7 helium stars and one 5-prong oxygen star. The general identification procedure is discussed and the arguments for the one 5-prong oxygen star are presented in some detail. Histograms of the $H\rho$ - and scatter-angle distributions of the star fragments are given.

The cloud chamber³ contained oxygen, helium, and water vapor with a total pressure of about half an atmosphere. The helium was introduced to minimize multiple scattering and to produce the low stopping power of 0.17 relative to air. Low stopping power was desirable in order to produce long tracks on which accurate curvature measurements could be made. The

¹ W. M. Brobeck, E. O. Lawrence, *et al.*, *Phys. Rev.* **71**, 449 (1947).

² R. Serber, *Phys. Rev.* **72**, 1007 (1947).

³ Brueckner, Hartsough, Hayward, and Powell, *Phys. Rev.* **75**, 555 (1948).